

# Effect of Pressure Swirl Atomizer Geometry on Spray Performance

Ibrahim I.A.<sup>1</sup>, Gad H.M.<sup>1</sup>, Baraya E.A.\*<sup>1</sup>, Farag T.M.<sup>1</sup>

<sup>1</sup>Mechanical Power Engineering Department. Faculty of Engineering, Port Said University,  
Port Said, Egypt

\*[eslam.ahmad@eng.psu.edu.eg](mailto:eslam.ahmad@eng.psu.edu.eg)

## Abstract

In the present study a modified pressure swirl atomizer is designed and manufactured to be suitable for a wide range of operating conditions. The spray performance of the modified pressure swirl atomizer is experimentally investigated under different internal atomizer geometry. The studied parameters are injection pressures which changed from 0.5 to 10 bar, the orifice length to orifice diameter ratio ( $L/D$ ) which taken as 0.22, 0.25, 0.27 and 0.29 ( $L$  is taken constant at 1 mm), spin chamber diameter ( $D_s$ ) which taken as 8, 10 and 12 mm, swirling passage size (width x depth) which varied as 1x1, 1.5x1.5, 2x2 and 2.5x2.5 mm and nozzle constant  $K$ , these parameters are studied at constant spin chamber angle ( $\theta$ ) of 90°. The spray performance such as spray shape, spray cone angle, radial spray concentrations, spray momentum and breakup length are studied under different operating and geometrical conditions using water as atomized liquid. The spray shape is photographed using digital camera to determine the spray cone angle and breakup length while the radial spray concentrations are measured by using the tubes patternator technique and the spray momentum is calculated from the spray concentration. An experimental test rig consists of fuel line, gear pump, valves and pressure gauges is used to study the spray performance at the above different operating conditions. An empirical formula for breakup length is developed in this work. A breakup length is measured experimentally to valid the results obtained of breakup length from digital photos. A comparison is carried out between the measured SCA with empirical equation for calculation SCA. The results indicated that by decreasing the size of swirl passage by about 60% the spray cone angle increased by about 50 %. It is also noticed that the breakup length decreased by about 51% when spin chamber diameter increased by about 33%.

## Keywords

Pressure swirl atomizers, fuel spray, breakup length, spray momentum.

## Introduction

Pressure-swirl atomizers are one of the simplest mechanical pressure atomizers that produce a hollow cone spray and are widely used in many applications, because it has many advantages over other atomizer types; simple construction, low cost, requirement small amount of energy for atomization and high reliability [1]. Pressure swirl atomizer sprays contain a wide range of droplet sizes and spray cone angles ranged from 30° to 150° depending on the application [2-4]. Pressure swirl nozzles have many design variations such as direction of liquid feeding which can be divided into axial and tangential flow design, Its geometry design has a significant effects in spray characteristics [5]. Pressure swirl atomizers has orifice diameter limitation; large orifices required large pump to delivered flow at high pressure to give good spray performance, small orifices make problem due to contaminates, deposits closed off the swirling ports due to soot formations at high combustion process [6]. Chung.Y et al [7] studied the effect of varying diameter, length of spin chamber and number of swirl tangential passage at the entry of spin chamber on the spray sheet film thickness. A geometrical parameter that is found to correlate with some performance parameters is the nozzle constant [1,8], which defined as

$$K = \frac{A_p}{D * D_s} \quad (1)$$

Xue et al. [8] studied numerically the effect of various geometrical parameters on the formation of the spray sheet, showing the effect of those parameters on the spray cone angle, film sheet thickness and discharge coefficient. The recommended swirl angle of  $\theta=90^\circ$  that created small recirculation region in the spin chamber, therefore increased the spray cone angle (SCA) and produce thin film thickness. Spray cone angle is considered one of most important parameters that evaluate the spray quality, estimation of average spray cone angle can be made by analysing the radial concentration distribution profiles. The boundary of the spray can be identified by determine the locus of the radial maximum points and the distance from the spray patterntation from the spray nozzle. Spray cone angle is affected with physical properties of tested liquid [9-12]. Liu Z. et al [13] studied experimentally air core size variation with spin chamber length and liquid viscosity.

Moon s. et al [14] estimated the breakup length of pressure swirl atomizer using analytically and experimentally. The phenomenon of jet breakup was quantified by measuring the breakup length, which is dependent on physical properties of atomizing liquid. Charalampous G. et al [15] measured the break up length of atomizing liquid spray with different methods; optical connectivity, electrical connectivity and shadowgraphs techniques. The difference between the three methods found to be within  $\pm 15\%$ . Spray momentum is considered a key factor that determining the rate of mixing of fuel and combustion air. Greeves G. et al [16] investigated experimentally the effects of nozzle geometry on spray momentum; the momentum efficiency is calculated experimentally from the measured spray momentum using force transducer with electrical output. Desantes.J. M. et al [17] measured experimentally the momentum under realistic operating condition; it is found that increase of momentum is proportional to the injection pressure. A force sensor is used to calculate the impact force of droplets using data acquisition system to record the change in voltage which calibrate as to indicate force.

The importance of studying the pressure swirl atomizer for different operating and geometrical conditions such as sprayed fluid properties, injection pressure spin chamber diameter, orifice diameter, entry port width and depth, length of the orifice is clearly appeared. In spray combustion application, the spray cone angle, breakup length, radial spray concentration distribution and spray momentum are very important characteristics which indicated improvement of the spray performance for increasing the combustion efficiency.

In the present study, the effects of geometrical parameters of modified pressure swirl atomizer such as  $L/D$ ,  $W \times H$ ,  $D_s$  and  $K$  on the spray performance at different operating conditions will be investigated. The design of modified pressure swirl atomizer is introduced to overcome the orifice limitation problem; liquid disintegration occurs through annulus orifice. The breakup measurements are validated by using different methods of measurement as presented in [25,26]. Spray performance of the modified pressure swirl atomizer will be studied for the following different conditions such as ( $L/D$ ) which taken as 0.22, 0.25, 0.27 and 0.29,  $W \times H$  which is varied as 1x1, 1.5x1.5, 2x2 and 2.5x2.5 mm,  $D_s$  which taken as 8, 10, 12 mm and nozzle constant  $K$  which is varied with variation of  $W \times H$ ,  $L/D$  and  $D_s$ . The spray shape, spray cone angle, radial spray concentration distribution, breakup length and spray momentum are studied for different operating conditions using water as atomization liquid, orifice length is constant in the study ( $L = 1$  mm) while orifice diameter is changed to get different  $L/D$  ratios, swirl angle  $\theta = 90^\circ$  is used in all experimental runs in this work.

### Experimental Test Rig

In order to study the effects of modified pressure swirl atomizer geometrical parameters  $L/D$ ,  $W \times H$  and  $D_s$  on spray performance, an experimental test rig consisting of liquid line, pressure swirl atomizer and the spray chamber is designed and manufactured. The layout of the experimental test rig is shown in Figure 1. The liquid line contains the liquid tank, liquid filter, liquid valve, gear pump, control valve, non-return valve and by-pass valve and ended by the pressure swirl atomizer which is centrally located in the spray chamber. The detailed dimensions of the used pressure swirl atomizer are shown in Figure 2. The fuel nozzle diameter ( $D$ ) is changed and the orifice length to orifice diameter ratio ( $L/D$ ) of 0.22, 0.25, 0.27 and 0.29 ( $L$  is constant at 1 mm). Fine spray droplets are generated inside the vertical cubic spray chamber which is of dimensions 50 cm x 50 cm with height of 70 cm. One side of the spray chamber is transparent to allow observation and taking images for the spray using the digital camera. The modified pressure swirl atomizer can be used as pressure swirl atomizer without using air inside air needle. In the present study, the spray is formed and exit through annulus area of the orifice. The atomizer is consisting of five parts; (1) atomizer body, (2) locking part to swirl fuel passage, (3) swirling part of fuel with different angles, (4) atomizer cap with different orifice diameters that contains spin chamber with cylindrical geometry and (5) central air needle. Liquid is issued from annulus area around the air needle with swirling motion.

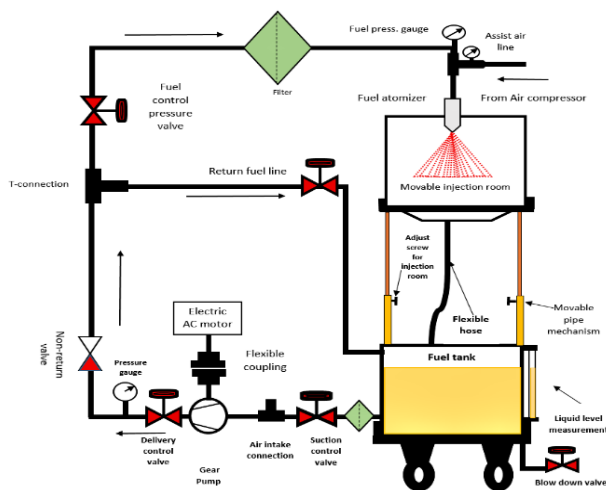


Figure 1. Layout of the experimental test rig.

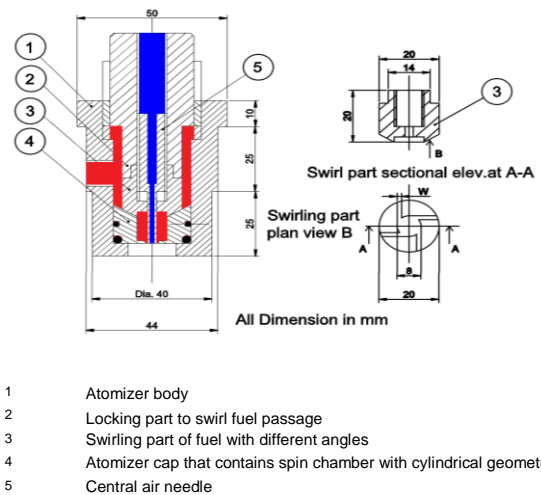


Figure 2. Detailed dimensions of the pressure swirl atomizer.

## Results and discussion

In this section, a series of experimental runs are carried out to investigate the effects of changing of  $L/D$ ,  $W \times H$  and  $D_s$ , on spray shape, SCA, radial spray concentration distribution (RSCD), spray momentum and breakup length. Water is used as atomized liquid in all experimental run.

### 1. Spray shape

Spray shape is one of the important parameter of spray; hollow cone shape is developed due to swirling motion of liquid in spin chamber of modified pressure swirl atomizer. The spray shape is changed with injected pressure and different geometrical parameters such as  $L/D$ ,  $D_s$  and  $W \times H$ . The spray is photographed to show spray shape variation with the injection pressure and consequently the spray cone angle under different operating conditions. Figure 3 shows the spray shape at different injection pressures. From the figure 3 it can be seen that, by increasing injection pressure the spray takes many shapes from screw shape, onion shape, tulip shape and fully developed spray shape. At low injection pressure the bulk liquid is not disintegrated, by increasing the injection pressure the liquid is fragmented to fine droplets in the final form of hollow cone shape. Figure 4 shows the effect of changing  $L/D$  on spray shape at injection pressure of 5 bar,  $\theta=90^\circ$ ,  $D_s=8$  mm and  $W \times H=1.5 \times 1.5$  mm<sup>2</sup>, from this figure it is observed that, by increasing  $L/D$  i.e. decreasing nozzle diameter, the spray envelope decreased and consequently cone angle decreased due to increase in spray momentum and so liquid penetration resulting in narrow cone angle longer penetration. Figure 5 shows the effect of changing spin chamber diameter at constant injection pressure and geometrical conditions on spray shape. By increasing the spin chamber diameter, the SCA increased due to increasing of swirling diameter that increased the angular rotation of liquid jet helping the spray to spread radially due to increasing of air core diameter. It is clearly appeared from figure 6 that, the SCA is affected by the swirl passage size. The liquid jet enters the spin chamber with high velocity at small dimension of swirl passage, it is known that  $v=\omega.r$  where  $\omega$  is angular rotation and  $r$  is radius of angular rotation, at constant radius the angular rotation increased and then SCA increased produce thin film thickness by decreasing swirl passage size.

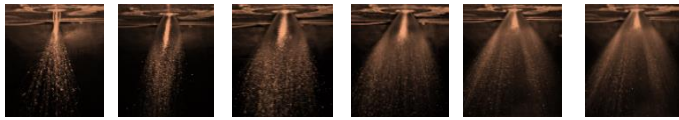


**Figure 3.** Effect of injection pressure on the spray shape at  $L/D = 0.25$ ,  $W \times H = 2 \times 2$ ,  $\theta = 90^\circ$  and  $D_s = 10$  mm.

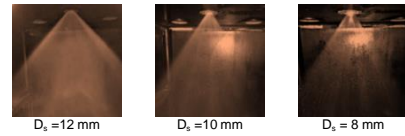


**Figure 5.** Effect of spin chamber diameter on the spray shape at  $P = 7$  bar,  $L/D = 0.29$ ,  $W \times H = 1.5 \times 1.5$  and  $\theta = 90^\circ$ .

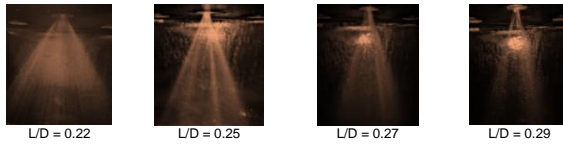


**Figure 4.** Effect of length to diameter ratio on the spray shape at  $P = 5$  bar,  $\theta = 90^\circ$ ,  $W \times H = 1.5 \times 1.5$  and  $D_s = 8$  mm.

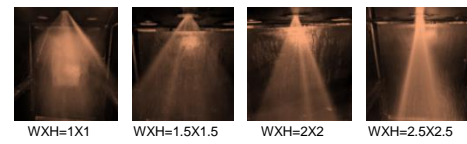


**Figure 6.** Effect of swirl passage width and depth on the spray shape at  $P = 6$  bar,  $L/D = 0.27$ ,  $\theta = 90^\circ$  and  $D_s = 10$  mm.

### 2. Spray cone angle

An important aspect of atomizer design is SCA, increasing of SCA leads to an increase in the exposure of the droplets to the surrounding air, which results in improved atomization. Increasing SCA improved atomization, combustion performance and pollutant emission [18,19]. The SCA are affected by the flow number of the atomizer orifice and the discharge coefficient of the orifice, flow number represent the effective flow area of the exit orifice. The effects of changing the geometrical parameters  $L/D$ ,  $W \times H$ ,  $D_s$  on the SCA are investigated at different injection pressures. The SCA are obtained from the spray photographs which are taken by digital camera, the photographs are processed in the AutoCAD software to indicate the spray cone angle, and the atomizing liquid used in experimental runs is water at ambient conditions. The uncertainty of measuring spray cone angle  $\pm 2\%$ . SCA may be estimated in dependence on the liquid properties and the atomizer dimensions by an empirical correlation of Lefebvre [22]:

$$SCA = 8.1(K)^{-0.39}(D)^{1.13}(\mu)^{-0.9}(\Delta P)^{0.39} \quad (2)$$

According to this equation, the spray cone angle is widened by increases in discharge orifice diameter, liquid density, and injection pressure, while it is diminished by an increase in liquid viscosity. The maximum error between theoretical and measured values is about 7%. The effect of changing the injection pressure on SCA is shown in Figure 7. It is noticed that, by increasing the injection pressure SCA increased as discussed by Ashgriz et al [20]. Increasing  $P_{inj}$  from 3 bar to 10 bar, the SCA increased by about 100%. The SCA increased by increasing injection pressure or liquid mass flow rate at different nozzle geometries. Figure 8 shows the effect of changing  $L/D$  on the SCA at different injection pressures. It is clearly inferred that, the SCA is decreased by increasing of  $L/D$  ratio for specified injection pressure. At  $P_{inj}$  of 3 bar the SCA increased by about 60% when  $L/D$  decreased from 0.29 to 0.22 (24 %). By increasing  $L/D$  i.e. decreasing orifice diameter, the discharge coefficient is decreased and thus the SCA

spread radially. At  $P_{inj}$  of 6, 8 and 9 bar the SCA increased by about 49%, 43% and 38%, respectively as  $L/D$  decreased from 0.29 to 0.22. The flow number is decreased with increasing the annuals area of the orifice at different injection pressures. The lower value of flow number corresponding to high swirling effect of orifice and increasing in SCA [2]. The effect of changing  $D_s$  on the SCA at different injection pressures is shown in Figure 9. It is obviously seen that, the SCA increased by increasing  $D_s$ . At  $P_{inj}$  of 5 bar the SCA increased by about 28% as the spin chamber diameter increased from 8 to 12 mm. For small diameter ( $D_s = 8$  mm) the SCA decreased at high  $P_{inj}$  (greater than 9 bar). The reduction in SCA is due to the increase of spin chamber back pressure resulting from increasing injection pressure with smaller spin chamber diameter. Effect of changing swirl passage dimensions  $W \times H$  on the SCA is presented in Figure 10. It is noticed that, swirl passage width and depth are most parameter that effect on the SCA. By increasing swirl passage dimensions ( $W \times H$ ), SCA significantly decreased. As the swirl passage size increased, the angular liquid velocity decreased at the entry of the spin chamber. The angular momentum of liquid decreased due to decreasing of angular liquid velocity in spin chamber. So, the spray sheet film thickness increased as a result of decreasing air core diameter and that leads to a decrease in the SCA. The effect of changing nozzle constant on the measured and calculated SCA at different injection pressures, is shown in figure 11. The figure shows that SCA is decreased as nozzle constant increased. The maximum error between the measured and calculated SCA from Lefebvre equation(calculated) is about 7%. Nozzle constant is increased as the orifice diameter decreased and all parameters still constant, thus SCA is decreased as indicated of Lefebvre [11].

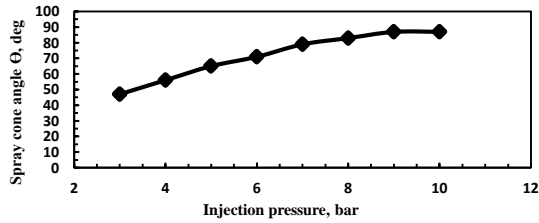


Figure 7. Effect of changing injection pressures on SCA at  $\theta = 90^\circ$ ,  $L/D = 0.27$ ,  $D_s = 10$ mm and  $WXH = 1.5 \times 1.5$ mm<sup>2</sup>.

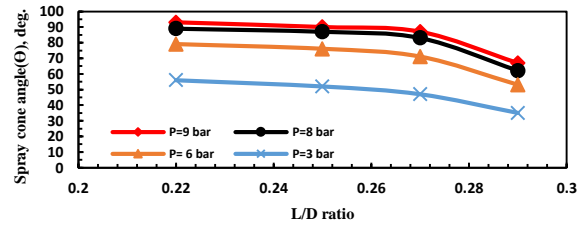


Figure 8. Effect of changing  $L/D$  on the SCA at  $\theta = 90^\circ$ ,  $D_s = 10$ mm and  $WXH = 1.5 \times 1.5$ mm<sup>2</sup>.

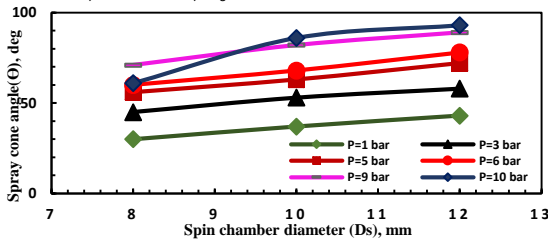


Figure 9. Effect of changing  $D_s$  on the SCA at  $\theta = 90^\circ$ ,  $L/D = 0.27$  and  $WXH = 1.5 \times 1.5$ mm<sup>2</sup>.

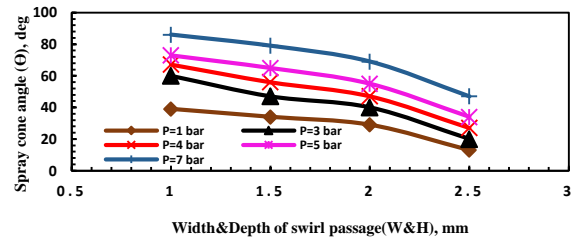


Figure 10. Effect of changing swirl passage dimensions ( $W \times H$ ) on the SCA at  $L/D = 0.27$ ,  $D_s = 10$ mm and  $\theta = 90^\circ$ .

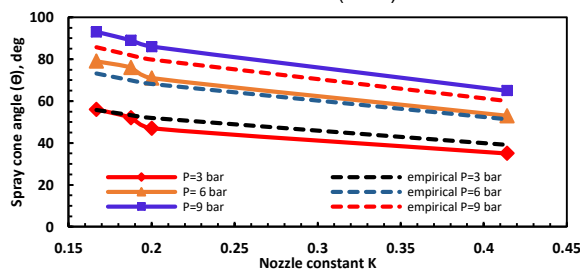


Figure 11. Effect of changing nozzle constant on the measured and calculated SCA at different injection pressures, at  $D_s = 10$ mm,  $A_p = 7.5$ mm<sup>2</sup>,  $WXH = 1.5 \times 1.5$  mm<sup>2</sup> and  $\theta = 90^\circ$ .

### 3. Spray concentration

One of simple methods of determining the atomizing liquid concentration distribution is by collecting the liquid spray in tubes. A spray pattarnator have some types such as inline pattarnator, sector pattarnator and radial or circle pattarnator. In this study, a circle pattarnator are used which consist of tubes arranged in half circle at various radial region of spray. The amount of the liquid in the tubes is measured to determine the spray liquid concentration at specific time. RSCD is measured by circle pattarnator of 37 cm radius consist of 19 tubes of 12 mm diameter. Circle pattarnator located at a specified constant radial distance of 14 cm from the atomizer exit. Before spray distribution measurements, the flow rate of each nozzle was tested by collecting the amount of liquid directly from the atomizer at different pressures for ten seconds and measuring nozzle output volume. Measurements were carried out at 25°C. The maximum error of all nozzles with nominal flow rate was  $\pm 3.5\%$ .

The effect of geometrical parameters length to diameter ratio, diameter of the spin chamber, and the swirl passage dimensions on the RSCD is carried out at different injection pressures. Figures 12-15 show the effects of studied parameters on the RSCD. Due to symmetrical radial distribution, half of the spray envelopes are presented. Figure 12 shows RSCD at different injection pressure and certain geometrical conditions of  $D_s = 10$  mm,  $W \times H = 2 \times 2$  mm<sup>2</sup>,  $\theta = 90^\circ$  and  $L/D = 0.27$ . It is clearly appeared that, the RSCD has one peak value at certain radius and has zero value at the spray centerline because the spray is hollow cone. As the  $P_{inj}$  increased the SCA is spread widely leads to a higher quality of atomization and better dispersion of liquid droplets. By increasing injection pressure, RSCD peak value decreased and shifted outward, the spray diameter increased as a result of SCA increased.

The effect of different length to diameter ratio  $L/D$  on RSCD is presented in Figure 13 at  $W \times H = 1.0 \times 1.0$  mm<sup>2</sup>,  $\theta = 90^\circ$  and  $D_s = 10$  mm RSCD and  $P_{inj}$  of 5 bar. It is clearly inferred that, by increasing the  $L/D$  ratio (decreasing the nozzle diameter). The maximum value of RSCD is increased and shifted toward to spray center, decreasing  $L/D$  ratio leads to increase in SCA due to increase in nozzle diameter. Increasing the nozzle diameter, the liquid velocity decreased leads to spray spread outwards. SCA decreases with drop of the orifice diameter as a result of increased discharge coefficient and decreasing in flow number of orifice.

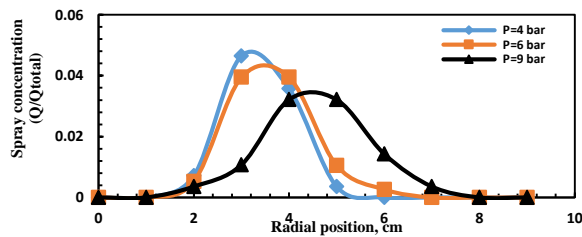


Figure 12. Effect of changing injection pressure on RSCD at  $D_s = 10$  mm,  $W \times H = 2 \times 2$  mm<sup>2</sup>,  $\theta = 90^\circ$  and  $L/D = 0.27$ .

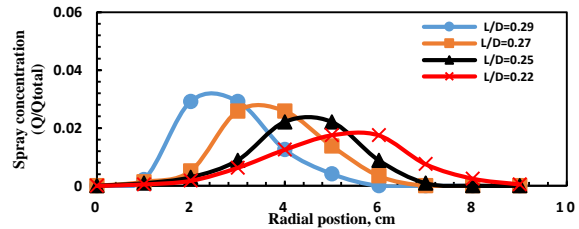


Figure 13. Effect of changing  $L/D$  ratio on RSCD at  $W \times H = 1.0 \times 1.0$  mm<sup>2</sup>,  $\theta = 90^\circ$ ,  $D_s = 10$  mm and  $P = 5$  bar.

Figure 14 indicates the effect changing spin chamber diameter on RSCD for a certain conditions of  $L/D=0.27$ ,  $W \times H = 1 \times 1$  mm<sup>2</sup>,  $\theta=90^\circ$  and  $P = 4$  bar. It can be seen that, at  $D_s = 10$  and 12 mm there are clear variation in the radial position of RSCD peak value but its value slightly decreased by decreasing spin chamber diameter. The peak value of RSCD is reduce and shifted radially toward the spray center as a result of decreasing in SCA at  $D_s = 8$  mm due to the increase of spin chamber back pressure.

The effect of swirl passage dimensions on RSCD is shown in Figure 15 for a certain conditions of  $L/D=0.27$ ,  $W \times H = 1 \times 1$  mm<sup>2</sup>,  $\theta=90^\circ$  and  $P = 4$  bar. It is obviously appeared that, at same injection pressure, by decreasing swirl passage dimensions the maximum RSCD is found at certain radial location, the peak value of RSCD shifts outward and the spray diameter increases. Changing the volume of swirl passage is strongly affected the RSCD. Increasing of  $W$  and  $H$  of swirl passage reduce the SCA, therefore RSCD is widely opened outward from spray center. An increase in spray diameter with decreasing swirl passage size from  $W \times H = 2.5 \times 2.5$  mm<sup>2</sup> to  $W \times H = 1 \times 1$  mm<sup>2</sup> due to thin film thickness of spray sheet, wide air core diameter and maximum SCA which increased the projected area of the spray cone.

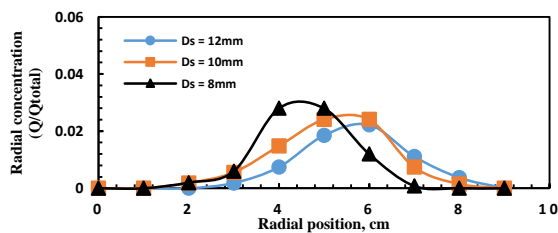


Figure 14. Effect of changing  $D_s$  on RSCD at  $L/D=0.27$ ,  $W \times H = 1 \times 1$  mm<sup>2</sup>,  $\theta=90^\circ$  and  $P = 4$  bar.

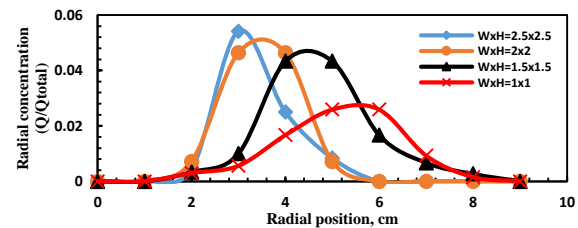


Figure 15. Effect of changing  $W, H$  of swirl passage  $D_s$  on RSCD at  $\theta=90^\circ$ ,  $n=19$ ,  $L/D=0.27$ ,  $h=14$  cm,  $D_s=10$  mm and  $P = 4$  bar.

#### 4. Spray breakup length

Jet breakup phenomenon of spray jet are affected by four important forces, inertia force, viscous force, surface tension and aerodynamic forces acting on the jet [20]. Surface tension is physical property that resists expansion of liquid surface area. Surface tension forces must be overcome by aerodynamic, centrifugal or pressure forces to achieve proper atomization. The breakup length is defined as the length from the spray nozzle to the end of continuous spray sheet. The common purpose of breaking a bulk liquid jet into spray is to increase the liquid surface area and decreasing the breakup length to minimum value so that subsequent heat and mass transfer can be increased. [21-24]. The break up length measured from the digital camera photos with uncertainty of  $\pm 4\%$ . The breakup length obtained from photos by digital camera is compared with that obtained by other experimental technique studied by [25,26] to validate our results and it gives good agreements. The maximum error between two methods is about 4%.

An empirical formula for break up length are obtained as a function in Reynolds number and nozzle constant of atomizer. The maximum error nearly about 3.6%. The empirical equation is,

$$L_b = \frac{1000}{Re * P_{inj}} e^{-(60 * Re + K * Z)} \quad (3)$$

where  $L_b$  break up length in mm,  $Re$  Reynolds number,  $P_{inj}$  injection pressure in bar and  $Z$  constant function in injection pressure. i.e. type of flow laminar or turbulent.

Figure 16 shows the effect of injection pressure on the breakup length. It is shown that, the  $L_b$  is reduced with increasing the injection pressure, the reduction of liquid  $L_b$  as a result of increasing Reynolds' number due to high liquid spread velocity. The breakup is decreased by about 100% by increasing the  $P_{inj}$  from 1 bar to 7 bar. As the spray is fully developed cone at  $P_{inj}$  of 7 bar the breakup length disappeared. The effect of length to diameter ratio on the breakup length is shown in Figure 17 at  $\theta=90^\circ$ ,  $L/D=0.25$  and  $D_s=10$  mm. It is clearly shown that, the  $L_b$  is proportional inversely with  $L/D$  ratio. By increasing  $L/D$  from 0.22 to 0.29, the breakup length is decreased by about 1600%, 630 % and 300 % at  $P_{inj}$  of 5, 3 and 1 bar respectively. This reduction is due to the decrease in orifice diameter which helps to disintegrate the liquid sheet into droplets. Increase in exit liquid velocity leads to an increase in the momentum force.

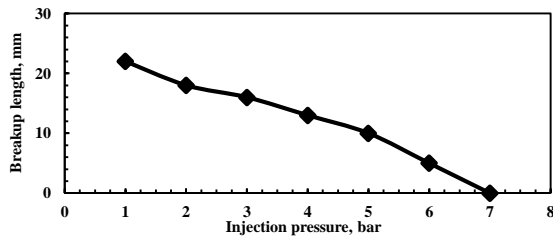


**Figure 16.** Effect of injection pressure on breakup length at  $\theta=90^\circ$ ,  $L/D=0.25$ ,  $D_s=10$  mm and  $W \times H=1.5 \times 1.5$  mm<sup>2</sup>.

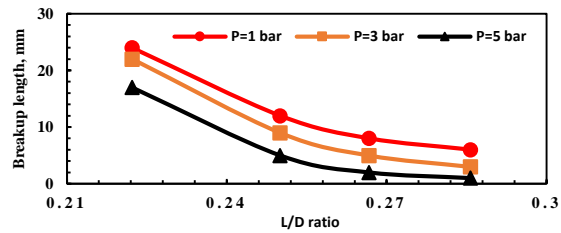


**Figure 17.** Effect of changing length to diameter ratio on breakup length at  $\theta=90^\circ$ ,  $D_s=10$ mm and  $W \times H=1.5 \times 1.5$  mm<sup>2</sup>.

Figure 18 shows the effect of changing injection pressure on breakup length at different spin chamber diameters at  $\theta=90^\circ$ ,  $L/D=0.27$  and  $W \times H=1 \times 1$  mm<sup>2</sup>. By increasing  $D_s$ , the breakup length is reduced, this is due to increasing of swirling effect by increasing spin chamber diameter. Increasing of  $D_s$  leads to increasing of angular momentum helps to break the bulk liquid into droplets and reduce the continuous liquid length. Continuous liquid length at  $D_s=12$  mm disappear at pressure of 4 bar while the continuous liquid is still existing at  $D_s=10$  mm at  $P=6$  bar.  $L_b$  decreased by about 48%, 44% and 100% by increasing  $D_s$  from 8 mm to 12 mm at  $P_{inj}=1, 2$  and 4 bar respectively. Effect of changing swirl passage dimensions on the breakup length at different injection pressures at  $\theta=90^\circ$ ,  $L/D=0.27$  and  $W \times H=1 \times 1$  mm<sup>2</sup> is shown in Figure 19. From this figure it can be seen that, by increasing swirl passage size spray  $L_b$  increased up to  $W \times H=1.5 \times 1.5$ , after that the breakup length decreased by increasing  $W \times H$  for all injection. For high injection pressure ( $>4$  bar) the  $L_b$  disappeared when swirl passage size increased to be  $2 \times 2$  mm, this is due to the spray becomes fully developed. Small swirl passage means increasing in flow velocity at the entry of spin chamber resulting in wide SCA. Large swirl passages have high penetration length due to narrow SCA and low breakup length. Figure 20. shows the effect of changing nozzle constant on the measured breakup length from digital camera at different injection pressures and empirical formula with dash lines. The  $L_b$  decreased with increasing the value of  $K$ , nozzle constant increased when the orifice diameter decreased. The spray jet velocity increased and this helps to disintegrate the liquid and minimize the breakup length.

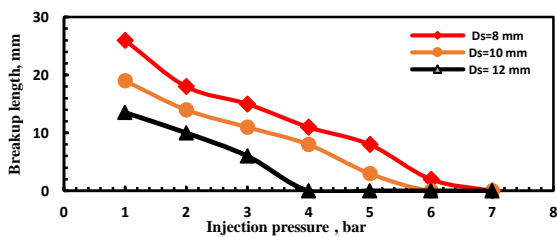


**Figure 18.** Effect of changing injection pressure on breakup length at different  $D_s$  at  $\theta=90^\circ$ ,  $L/D=0.27$  and  $W \times H=1 \times 1$  mm<sup>2</sup>.

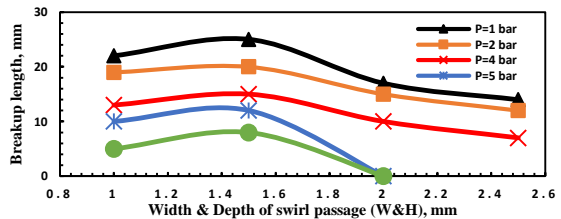


**Figure 19.** Effect of changing swirl passage dimensions ( $W \times H$ ) on the breakup length at  $\theta=90^\circ$ ,  $L/D=0.25$  and  $D_s=10$

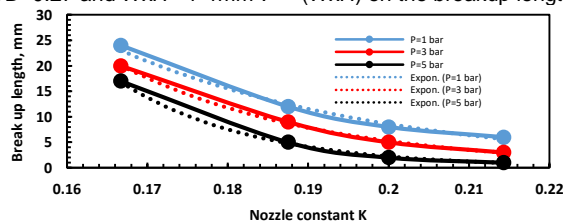


**Figure 20.** Effect of changing nozzle constant on the measured and calculated breakup length at different injection pressures, at  $\theta=90^\circ$ ,  $D_s=10$ mm and  $W \times H=1.5 \times 1.5$  mm<sup>2</sup>.

## 5. Spray momentum

Spray momentum can be measured by directing the fuel spray on to a fixed plate that is arranged to measure the impact force on the plate necessary to destroy all of the axial momentum in the fuel spray/jet [16]. The spray momentum is an important factor which indicates the penetration of the spray inside the combustion chamber. Spray momentum play significate role in mixing and air fuel ratio, therefore affect soot formation in combustion process. The spray momentum would be investigated to increase its penetration to get good mixing with combustion air and avoid impingement onto combustor walls.

In the present work the spray momentum is studied under different geometrical parameters and calculated using the results from radial spray concentration as calculated in [27]. The flow velocity of each tube is calculated by indicating the cross section area of single tube from the collected liquid in each tube. Figure 21 shows effect of changing L/D ratio on the spray momentum at  $\theta=90^\circ$ ,  $D_s=10$  mm,  $WXH=1.5 \times 1.5$  mm and  $P=5$  bar. It can be seen that, the peak value of momentum is increased by decreasing the L/D ratio (increasing the nozzle diameter) and shifted outward due to an increase in exit velocity and spray cone angle. L/D ratio is considered the most parameter that affects the spray momentum and its position from the spray center. Effect of swirl passage size (W&H) on the spray momentum is shown in Figure 22 at  $\theta = 90^\circ$ ,  $D_s = 10$  mm,  $L/D = 0.27$  and  $P = 4$  bar. It is obviously seen that, the peak value of spray momentum is increased by reducing  $W \times H$ , the maximum value of momentum is at  $W \times H = 1 \times 1$  mm<sup>2</sup>. The peak value of spray momentum is shifted outward from spray center by decreasing swirl passage size. Increasing  $W \times H$  from  $1 \times 1$  to  $2.5 \times 2.5$  mm<sup>2</sup> the peak momentum reduced by about 50% and its position from spray center reduced by about 50%.

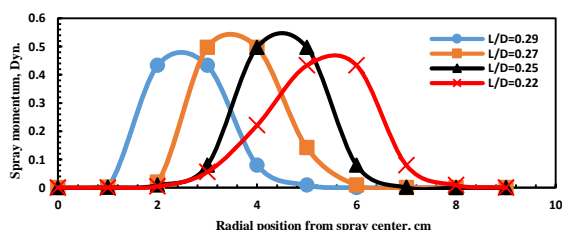


Figure 21. Effect of L/D ratio on the spray momentum at  $\theta=90^\circ$ ,  $D_s=10$  mm,  $WXH=1.5 \times 1.5$  mm and  $P=5$  bar.

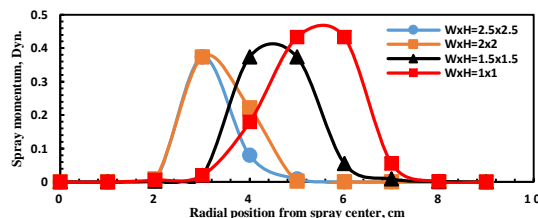


Figure 22. Effect of swirl passage size on the spray momentum at  $\theta=90^\circ$ ,  $D_s=10$  mm,  $L/D=0.27$  and  $P=4$  bar.

## Conclusions

From the experimental results of the present work the parameters changed are length to diameter ratio  $L/D = 0.22, 0.25, 0.27$  and  $0.29$ , swirl passage width and depth  $W \times H = 1 \times 1$  mm<sup>2</sup>,  $1.5 \times 1.5$  mm<sup>2</sup>,  $2 \times 2$  mm<sup>2</sup> and  $2.5 \times 2.5$  mm<sup>2</sup> spin chamber diameter  $D_s = 8, 10$  and  $12$  mm at different injection pressure. The nozzle constant is changed with varying the geometrical parameters of  $A_p$ ,  $D_s$  and  $D$ . Experiments were carried out to measure the break up length, an empirical formula was obtained for calculate break up length for spray jets. The SCA are measured at different operation conditions and are compared with Lefebvre SCA empirical equation with maximum error of 7% from actual measured value. The following conclusions for main results can be summarized:

- I. There are good agreements between the obtained experimental results of SCA and theoretical results from empirical equation (2).
- II. There are good agreements between the obtained experimental results of breakup calculation methods and theoretical devolved empirical equation (3) for breakup length.
- III. By increasing L/D ratio, the SCA, breakup length and maximum RSCD decreased, the maximum spray momentum and RSCD are radially shifted toward the spray centre.
- IV. By increasing K from 0.167 to 0.215,  $L_b$  decreased by 700%, 400%, 240% at  $P_{inj}$  of 5, 3, 1 bar respectively.
- V. At  $P_{inj}$  of 6, 8 and 9 bar the SCA increased by about 49%, 43% and 38% respectively as L/D decreased from 0.29 to 0.22.
- VI. By increasing L/D from 0.22 to 0.29 the  $L_b$  is decreased by about 1600%, 630 % and 300 % at  $P_{inj}$  of 5, 3 and 1 bar respectively.
- VII. By increasing spin chamber diameter ( $D_s$ ), the SCA increased,  $L_b$  decreased, RSCD is shifted radially outward. At  $P_{inj}$  of 5 bar the SCA increased by about 28% as the spin chamber diameter increased from 8 to 12 mm.  $L_b$  decreased by about 48%, 44% and 100% by increasing  $D_s$  from 8 mm to 12 mm at  $P_{inj}= 1, 2$  and 4 bar respectively.
- VIII. By increasing K from 0.167 to 0.42, SCA decreased by 43%, 49%, 39% at  $P_{inj} = 9, 6, 3$  bar respectively.
- IX. By increasing swirl passage width and depth, the SCA,  $L_b$ , peak value of spray momentum and maximum RSCD decreased. RSCD and maximum spray momentum are shifted toward spray centreline.  $L_b$  is decreased by about 57%, 58.3% and 85% with increasing  $W \times H$  from  $1 \times 1$  mm<sup>2</sup> to  $2.5 \times 2.5$  mm<sup>2</sup>.
- X. By increasing the  $P_{inj}$  for all atomizer geometry, the SCA increased, RSCD is shifted outward from spray centre, breakup length decreased.

## Acknowledgements

The authors are grateful to the employees of laboratories of the Faculty of Engineering, Port Said University.

## Nomenclature

L	orifice length [mm]	$\Theta$	spray cone angle [deg.].
D	orifice diameter [mm]	h	height from spray patteration to orifice [cm].
W	width of swirl passage [mm]	$D_s$	spin chamber diameter [mm].
H	depth of swirl passage [mm]	n	no. of tubes of spray paternattion.
$\varnothing$	swirl angle of fuel [deg.]	DC	direct current.
SCA	spray cone angle [deg.]	RSCD	radial spray concentration distribution.
L/D	length to diameter ratio.	$\omega$	angular rotational.
$A_p$	total area of tangential entry ports.	K	nozzle constant.
$L_b$	break up length [mm]	$\mu$	absolute viscosity [pa.s]
$P_{inj}$	injection pressure	$Re$	Reynolds number

## References

- [1] H. Lefebvre and Vincent G. McDonell, 2016, "Atomization and Sprays."
- [2] Loana Laura Omocea, Claudiu, Mihaela Turcanu, Corneliu Balan, 2016, Energy Procedia, Vol. 85, pp. 383-389
- [3] Milan Maly, Lada Janackova, Jan Jedelsk, Jaroslav Slama, Marcel Sapik, Graham Wigley, 2017, ILASS–Europe 2017, 28th Conference on Liquid Atomization and Spray Systems, Valencia, Spain.
- [4] Uzair Ahmed Dar, Mykola Bannikov, 2014, International Journal of Fluid Mechanics Research, Vol. 41, Issue 1, pp. 51-70.
- [5] Abhijeet Kumar and Srikrishna Sahu, 2018, International Journal of Spray and Combustion Dynamics 0(0) 1–20.
- [6] Jan Jedelský, Milan Malý, Lada Janáčková, Miroslav Jícha, 2016, ILASS – Europe, 27th Annual Conference on Liquid Atomization and Spray Systems, Brighton, UK
- [7] Yunjae Chung, Hyuntae Kim, Seokgyu Jeong, Youngbin Yoon, 2016, , journal of propulsion and power.
- [8] J. Xue, M. A. Jog, S. M. Jeng, 2004, International Journal of Hydrogen Energy, Vol. 41, Issue 35, 21, pp. 15790-15799
- [9] Muhammad Rashad, Huang Yong, Zheng Zekun, 2016, International Journal of Hydrogen Energy, Volume 41, Issue 35, pp.15790-15799
- [10] T. Marchione, C. Allouis, A. Amoresano, Federico Beretta, 2007, journal of propulsion and power, Vol. 23, No. 5., pp.1096-1101.
- [11] Reza Alidoost Dafsari, Hyung Ju Lee, Jeongsik Han, Dong-Chang Park, Jeekeun Lee, 2019, Fuel, Vol. 240, pp. 179-191.
- [12] A. Amoresano, C. Allouis, M. Di Santo, P. Iodice, G. Quaremba, V. Niola, 2018, Experimental Thermal and Fluid Science, Volume 94, pp.122-133.
- [13] Zhilin Liu, Yong Huang, Lei Sun, 2017, "Studies on air core size in a simplex pressure-swirl Atomizer."
- [14] Seoksu Moon, Choongsik Bae, Essam Abo serie, 2009, Atomization and Sprays, 19(3), pp. 235-246.
- [15] Charalampous. G, Constantinos Hadjiyiannis, Yannis Hardalupas, 2016, Measurement, vol.89, pp 288–299
- [16] Godfrey Greeves, Gavin Dober, Simon Tullis, Nebojsa Milovanovic, Stefan Zuelch, 2008, ILASS 2008, Sep. 8-10, ComoLake, Italy.
- [17] J. M. Desantes, R. Payri, F. J. Salvador, J. Gimeno, 2003, SAE International, ISSN 0148-7191.
- [18] Lefebvre, A. H., and Ballal, D. R., 2010, "Gas turbine combustion alternative fuels and emissions."
- [19] R.J. Kenny, James R. Hulka, Marlow D. Moser, Noah O. Rhy, 2009, journal of propulsion and power, Vol. 25, No. 4, pp.902-913.
- [20] Ashgriz, N, 2011, "Handbook of atomization and sprays theory and applications."
- [21] Debanik Bhattacharjee, 2013, International Journal of Engineering Research and Technology, ISSN 0974-3154 Volume 6, Number 6(2013), pp. 727-732
- [22] H. Lefebvre and Dilip R. Ballal, 2010, "Gas Turbine Combustion."
- [23] J.T.Yang, A.C.Chen, S.H.Yang, and K.J. Huang, 2003, PSFVIP-4 , F4052
- [24] Arash Zandian, William A. Sirignano, Fazle Hussain, 2018, International Journal of Multiphase Flow, v2, pp1706.03150
- [25] T.M. FARAG, 1992, port-said Scientific engineering bulletin, Vol.4, No.2, pp.175-188.
- [26] Hiroyasu, H., Shimizu, M. and Arai, M., 1982, 2nd ICLASS, PP.69-74.
- [27] Gad H. M., Ibrahim I. A., Abdel-baky M.E., Abd El-samed A. K., Farag T. M., 2019, IOSR Journal of Mechanical and Civil Engineering, Volume 16, Issue 2 Ser., pp. 69-77.